THE PROINFLAMMATORY EFFECT OF STRUCTURALLY ALTERED ELASTIC FIBERS IN A HAMSTER MODEL OF COPD EXACERBATION

A dissertation submitted in partial fulfillment
of the requirements for the degree of

DOCTOR OF PHILOSOPHY

to the faculty of the

DEPARTMENT OF GRADUATE DIVISION

of

COLLEGE OF PHARMACY AND HEALTH SCIENCES

at

ST. JOHN'S UNIVERSITY
New York
by
Shadi Mehraban

Date Submitted: 07/16/2020 Date Approved: 07/16/2020

Shadi Mehraban Dr. Jerome Cantor

ABSTRACT

THE PROINFLAMMATORY EFFECT OF STRUCTURALLY ALTERED ELASTIC FIBERS IN A HAMSTER MODEL OF COPD EXACERBATION

Shadi Mehraban

To further understand the effect of superimposed lung inflammation on COPD, our laboratory developed a hamster model of COPD exacerbations using sequential intratracheal instillations of lipopolysaccharide (LPS) and elastase. Using this model, the superimposed inflammatory effect of LPS on elastase-induced emphysema was studied through morphological and biochemical parameters. Total leukocyte and percent neutrophil count in bronchoalveolar lavage fluid (BALF), and elastin-specific desmosine crosslinks (DID) were measured 48 hours after LPS treatment. Morphometric changes were evaluated with mean linear intercept (MLI) methods, and interstitial elastic fiber and lung surface area measurements 1 week post-LPS treatment. Compared to controls, animals treated with elastase/LPS showed a significant increase in BALF leukocytes (187 vs 47.7 x 104 cells), neutrophils (39 vs 4.8 percent), and free DID levels (182 vs 97 percent). Additionally, MLI was significantly elevated in the elastase/LPS group compared to controls (156.2 vs 81.7micrometer). Due to enhanced splaying and fragmentation of elastic fibers, interstitial elastic fiber surface area was significantly increased in animals treated with elastase/LPS

than controls (49 vs 26 percent). On the other hand, lung surface area was decreased in elastase/LPS group compared to controls (17.8 vs 25.5 percent). Furthermore, intratracheal instillations of elastin peptides and LPS demonstrated significant effects on BALF neutrophils, free DID levels and leukocyte chemotactic properties. The results suggest that structural alterations in elastic fibers during exacerbations make them more susceptible to breakdown and may have a proinflammatory effect further accelerating loss of lung parenchyma and function.

ACKNOWLEDGEMENTS

First and foremost, I would like to thank my mentor, Dr. Cantor. This project would have not been possible without his continuous guidance and great support.

I would like to thank Dr. Wurpel, Dr. Reznik, Dr. Schanne, and Dr. Cerreta for serving as committee members on my doctoral defense, and for their valuable advice on completion of this project.

I owe my deepest gratitude to my parents and sister for their consistent support, care and encouragement throughout the years. To my friends, thanks for being there when I needed you the most. And to George, my labmate, thanks for all your help and support in conducting the experiments.

Finally, I would like to thank the Department of Pharmaceutical Sciences for resources and financial support.

TABLE OF CONTENTS

LIST OF TABLES

LIST OF FIGURES

Chapter 1: INTRODUCTION

Chronic obstructive pulmonary disease (COPD), characterized by progressive and irreversible airflow obstruction, exhibits the pathogenic features of emphysema, chronic bronchitis and/or asthma (1,2). Emphysema is characterized by gradual destruction of lung tissue, specifically thinning and elimination of alveolar walls with subsequent enlargement of air spaces (3). Chronic bronchitis is characterized by excess production of mucus by goblet cells increasing inflammation and obstruction of the airways (4). COPD is the third leading cause of death in the United States (5). Cigarette smoke is the primary cause of COPD with lifelong smokers having a 50% chance of developing the disease in their lifetime (6). Occupational exposure to dust, gases, fumes and silica can also cause COPD (7,8). Smoking cessation reduces the risk of COPD development by half (6). Smoke induces inflammatory responses in the lungs by recruiting oxidants, proteases and immune cells which contributes to expiratory airflow restriction (2). Smoke can also inhibit or alter the repair process of the lung parenchyma leading to destruction or fibrosis of the lung tissue, respectively (2). Tissue remodeling in small airways has also been detected in COPD patients (9). Additionally, persistent infiltration of inflammatory cells, including neutrophils, macrophages, T- and B- lymphocytes in the alveolar walls has been significantly associated with the severity of airflow obstruction based on Global Initiative for Chronic Obstructive Lung Disease (GOLD) criteria (10). The link between small airway obstruction and tissue remodeling in COPD patients remains uncertain.

1.1 Acute Exacerbations

Acute exacerbations of COPD (AECOPD) are defined by sudden aggravation of both respiratory and non-respiratory symptoms of COPD (11). Respiratory symptoms include cough, dyspnea and wheezing while non-respiratory symptoms include fatigue and malaise. Characteristics of AECOPD include bronchoconstriction, persistent cough, increased sputum production, and subsequent dyspnea (12,13). AECOPD have been associated with an accelerated decline in lung function and poorer prognosis in response to the increased inflammation in airways and lung parenchyma, especially in cases with mild COPD (14,15). The majority of episodes of AECOPD are initiated by a bacterial or viral respiratory infection, with non-typeable Hemophilus influenzae being the most common pathogen (13). They can also be caused by environmental air pollutants (16). The frequency of AECOPD episodes is increased as COPD progresses (17). The mechanisms underlying COPD exacerbations remains unknown (18). It is crucial to rule out congestive heart failure, pneumonia, and pulmonary emboli when COPD exacerbation is suspected (13). COPD exacerbations also accelerate the progression of emphysema, however, the underlying mechanisms leading to structural alterations in alveolar walls remains unknown (19).

1.2 Therapeutic Agents

The progressive decline in lung function in COPD is poorly reversible since no therapeutic agents or procedures studied to date have been effective in slowing down the progression of the disease other than smoking cessation or occupational exposure discontinuation (20). Therefore, the main objective of pharmacological treatments available is to prevent or alleviate the symptoms, and decrease the frequency and severity of AECOPD (21). The most common anti-inflammatory agents used in COPD are corticosteroids (22). However, corticosteroids show poor efficacy in severe cases of COPD (23,24). Despite showing efficacy in exacerbations of COPD, glucocorticoids are generally not used in stable COPD due to their side effects and high costs (21). Additionally, corticosteroid resistance remains a challenging topic in treating severe COPD (22). Another centerpiece of COPD symptomatic treatment is bronchodilators including short-acting and long-acting β2-agonists, anticholinergic antimuscarinic agents, and theophylline (21). Mucolytic agents have also proved to be effective in reducing the frequency of AECOPD (25).

1.3 Elastic Fibers

A major component of elastic fibers is elastin which plays a critical role in the biomechanics of the lungs permitting passive tissue recoil (elastic recoil) during expiration. These bundles of protein found in the extracellular matrix (ECM) of the connective tissue are mainly produced by fibroblasts, smooth muscle cells,

chondrocytes and endothelial cells (26). Elastases are a group of enzymes that break down elastic fibers and are produced in various locations, including pancreas, neutrophils, macrophages and platelets (26). Elastin degradation is a principal stage in the pathogenesis of COPD (27). Intratracheal (IT) instillation of elastase can promptly result in an approximate 40% loss of elastin in the lung mimicking emphysema (26,28). Enzymatic and oxidative breakdown of elastic fibers, producing elastin fragments, results in recruitment of inflammatory cells, including neutrophils, macrophages and lymphocytes to the lung which further aggravates elastic fiber degradation and loss of lung parenchyma and function (27). The main hypothesis for the development and progression of COPD and primarily emphysema is the protease-antiprotease imbalance (29). The protease-antiprotease imbalance theory has mainly been studied in patients with alpha-1 antitrypsin deficiency who lack the alpha-1 antitrypsin, a neutrophil elastase inhibitor, leading to irreversible alveolar wall destruction and emphysema (30). Elastin degradation in COPD eventually contributes to loss of lung recoil causing a greater strain on alveolar walls (29). This mechanical failure in the interrelated lung parenchymal network leads to uneven distribution of forces in alveolar walls further deteriorating airspace enlargement and rupture (31).

1.4 Desmosine and Isodesmosine

Elastin cross-linking in the lung consists of two amino acids unique to mature elastin; desmosine and its isomer isodesmosine (DID) which can be used as a

biomarker of elastin degradation in COPD (32). DID are important diagnostic tools in evaluating the efficacy of drugs designed to decrease elastin degradation in COPD as they are reflective of enhanced elastic fiber turnover (32). Labib et al. reported an increased level of blood DID in stable COPD with a more enhanced elevation in AECOPD which determines greater lung destruction and further decline in lung function during exacerbations (33). Another study by Kim et al. found an association between urinary desmosine levels and the severity of emphysema (34). Recruitment and activation of inflammatory cells induced by smoking or AECOPD ,especially neutrophils are also responsible in elevation of DID (33).

1.5 Lipopolysaccharides

Lipopolysaccharides (LPS), also known as endotoxins, are large molecules consisting of a lipid and polysaccharide with an O-antigen, and an outer and inner core. LPS which is found in the outer membrane of gram negative bacteria is present in cigarette smoke in considerable amounts as well as various occupational and environmental hazards (35,36). Inhaled LPS acts as a pro-inflammatory agent causing a surge in neutrophils, macrophages and cytokines in the sputum and bronchoalveolar lavage fluid, which can further lead to bronchoconstriction (37).

Total leukocyte and neutrophil counts were significantly increased after inhalation of LPS in blood and sputum of healthy human subjects (38). Brass et al. observed

emphysematous changes in the lungs of experimental mice for up to 4 weeks after inhaling LPS which can be attributed to apoptosis (39). Furthermore, Lee et al. reported histopathological changes in the lungs as well as significant elevations in leukocyte and neutrophil counts in bronchoalveolar lavage fluid (BALF) of mice, 48 hours after intranasal instillation of LPS (40). A single dose of IT LPS instillation in mice with elastase-induced emphysema mimics a human case of COPD exacerbation with more prominent alveolar destruction and inflammatory cell infiltration compared to elastase alone, LPS alone or control groups (18). Additionally, inhalation of nebulized LPS in guinea pigs resulted in inflammatory cells accumulation, goblet cell hyperplasia and alveolar enlargement in the lungs (41). Intranasal exposure to elastase and LPS in mice also led to decreased lung recoil, airway inflammation and obstruction, and goblet cell metaplasia (35).

1.6 Elastin Peptides

Elastin peptides (EP) in COPD patients are products of elastic fiber degradation by proteases, especially neutrophil proteases. Dupont et al. found that plasma concentrations of EP are elevated in stable COPD and twofold greater in COPD exacerbations. They also reported neutrophils to be unresponsive to EP which could be attributed to downregulation of elastin receptors of neutrophils during exacerbations (42).

1.7 Chemotaxis Assay

Chemotaxis studies assess the ability of different cells to migrate towards a chemical concentration gradient. The chemotactic activity of neutrophils has shown to increase during acute exacerbations of COPD (43). Furthermore, Wu et al. demonstrated increased neutrophil chemotaxis towards sputum of COPD patients which was correlated with COPD progression (44). However, Yoshikawa et al. detected reduced chemotaxis of neutrophils in sputum of COPD patients suggesting that COPD stages are not associated with increased cellular activity (45).

1.8 Terminal Deoxynucleotide Transferase Mediated dUTP nick end labeling (TUNEL Assay)

TUNEL assay is a procedure to detect apoptotic cells by identifying DNA fragmentation. An enzyme called terminal deoxynucleotide transferase catalyzes the attachment of dUTP nucleotides to the free 3'-hydroxyl termini of DNA breaks. Several studies have shown an increase in the apoptosis of the structural lung cells in COPD which may play a major role in the pathogenesis of the disease by correlating with alveolar destruction and airspace enlargement in emphysema (46–48). Additionally, apoptosis of neutrophils in COPD patients was significantly higher compared to controls with a positive correlation with lung function (49).

1.9 Summation

The underlying mechanisms of the pathogenesis and progression of COPD exacerbations and the role of elastic fibers in this process are not well understood. In order to study the effect of superimposed inflammation on elastic fiber injury in COPD exacerbation, our laboratory developed a novel hamster model of COPD exacerbation by LPS instillation to enhance elastase-induced emphysema. Contrary to previous models, this one uses a minimum dose of elastase to develop emphysema followed by a single dose of IT LPS to stimulate superimposed inflammation as in COPD exacerbation.

1.10 Hypotheses and Specific Aims

- Structural alterations in lung elastic fibers following elastase injury may increase their susceptibility to breakdown by secondary inflammation induced by LPS production.
- Elastin peptides released by these structurally altered elastic fibers may intensify the adverse effects of COPD exacerbations.
- Elastin degradation accompanying LPS infection may give rise to increased apoptosis and poorer outcomes of COPD exacerbations.

Aim 1: To test the first hypothesis, we determined the effect of elastase pretreatment on LPS-induced infiltration of inflammatory cells into the lungs,

lung parenchymal destruction and elastic fiber injury. This was evaluated by measuring the following parameters:

a) Total leukocyte count in BALF
b) Percent neutrophil count in BALF
c) Total and free DID content in BALF
d) Total lung DID content
e) Percent lung surface area
f) Percent interstitial elastic fiber surface area
g) Mean linear intercept
h) Internal surface area

Rationale: The number of leukocytes and neutrophils in BALF following LPS treatment demonstrates the extent of inflammation in the lungs which would help understand the complex pathogenesis of COPD exacerbations.

BALF DID content indicates the amount of elastic fiber breakdown after LPS instillation and the subsequent levels of elastin peptides which could be useful for understanding the pathophysiology of elastin degeneration during COPD exacerbations.

Lung surface area percentage is indicative of the extent of lung parenchymal destruction following LPS administration which may help describe why exacerbations are associated with a poorer prognosis of COPD. Interstitial elastic fiber surface area represents the amount of elastic fiber breakdown and the level of breakdown products (EP) in the lungs which may be helpful in explaining the progressive deterioration of lung function following exacerbations.

Aim 2: To test the second hypothesis, we assessed the effect of exogenously administered elastin peptides on LPS-induced infiltration of inflammatory cells into the lungs, lung parenchymal destruction and elastic fiber injury. This was evaluated by measuring the following parameters:

a) Total leukocyte count in BALF

b) Percent neutrophil count in BALF

c) Total and free DID content in BALF

Rationale: The number of inflammatory cells and neutrophils in the lungs after EP instillation would reveal whether these peptides have pro-inflammatory effects in the lungs which may lead to the irreversible aggravation of COPD symptoms following exacerbations. BALF DID levels indicate the degree of lung destruction after EP administration which may help explain the progressive decline in lung function following exacerbations.

Aim 3: To further test the second hypothesis, we determined the effect of LPS and elastin peptides, separately and in combination, on the chemotactic activity of leukocytes from untreated animals in vitro. This was evaluated by performing chemotaxis assay to measure the relative fluorescence of leukocytes in presence of LPS and peptides.

Rationale: The chemotactic activity of leukocytes towards a mixture of LPS and elastin peptides would be helpful in understanding exacerbations by showing whether structurally altered elastic fibers are responsible for the progression of the disease.

Aim 4: To test the third hypothesis, we determined the effect of elastase pre-treatment on LPS-induced apoptosis. This was evaluated by performing TUNEL assay to measure the number of apoptotic cells following treatment.

Rationale: The number of apoptotic cells following elastase pretreatment may further elucidate the complex pathogenesis of COPD exacerbations and the possible interesting role of apoptosis in the irreversible lung damage following exacerbations.

Chapter 2: Materials and Methods

2.1 Experimental Design

The following experimental protocols were used to determine the proinflammatory effect of structurally altered elastic fibers in COPD exacerbations.

Model 1

Syrian female hamsters were divided into four groups and treated as follows: Group 1 received IT instillation of 1unit porcine pancreatic elastase (Elastin Products, Owensville, MO), followed by 100 µg LPS (Sigma-Aldrich, St Louis, MO) 1 week later; Group 2 received IT instillation of 1unit elastase, followed by IT normal saline (NS) 1 week later; Group 3 received IT NS, followed by 100 µg LPS 1 week later; Group 4 received two IT instillations of NS with a 1 week interval (controls).

Morphometric measurements were made 1 week post-LPS treatment, including mean percent surface area of the lungs and interstitial elastic fibers, mean linear intercept (MLI) to determine airspace size, and internal surface area (ISA) per unit volume. Other measurements including, 1) total leukocyte count in BALF, 2) percent neutrophils in BALF 3) free and total BALF DID 4) total lung DID were performed 48 hours after LPS instillation, when lung inflammation was maximal.

Model 2

In another set of experiments, Syrian female hamsters were divided into four groups and treated as follows: Group 1 received a combination of 100 µg IT LPS and 50 µg lung elastin peptides (Elastin Products, Owensville, MO); Group 2 received 100 µg IT LPS alone; Group 3 was given 50 µg IT lung elastin peptides alone, and group 4 received IT NS alone. Measurements of 1) total leukocyte count in BALF 2) percent neutrophils in BALF 3) free and total BALF DID were made 48 hours after LPS and/or elastin peptides instillations. Additionally, chemotactic properties of elastin peptides and LPS (separately and combined) were examined using BALF leukocytes from untreated animals in a Boyden chamber assay.

2.2 Materials and Methods

2.2.1 Intratracheal Instillations

Female Syrian hamsters, with an approximate weight of 100 g, were anesthetized using an intraperitoneal (IP) injection of ketamine and xylazine (Henry Schein Animal Health, Dublin, OH) with a dose of 150mg/kg and 10mg/kg, respectively. The animal was monitored for a minimum of 10 minutes to confirm anesthesia. They were then laid supine on a surgical board and restricted by elastic bands

across their limbs. The cervical area was disinfected with 70% alcohol and a 2 cm vertical incision was made through the skin, subcutaneous fat and muscle tissue. The trachea was exposed and a 1ml syringe with a 27-gauge needle (BD PrecisionGlide Needle), bent to facilitate insertion, was introduced into the trachea. Following insertion, 0.2 ml of NS containing the agents described in the experimental design were injected into the lungs. After instillation of the compound and withdrawal of the needle from the trachea, the incision site was closed using several metal clips and topical lidocaine gel was applied as a topical anesthetic to decrease pain and discomfort in the surgical area. The animals were observed for a minimum of an hour until consciousness was regained. All the animals were then returned to their respective cages and were allowed free access to rodent chow and water ad-libitum.

2.2.2 Collection of Bronchoalveolar Lavage Fluid and Lung Samples

Animals were euthanized by CO_2 asphyxiation. The lower thoracic area was then cleansed with 70% alcohol and surgically exposed to cut the diaphragm, ensuring complete lung collapse. An incision was made in the cervical area and two muscle layers (cleidomastoedus and digastricus) were split to expose the trachea. The trachea was cannulated with a 16-gauge needle (BD PrecisionGlide Needle) attached to a 5ml syringe. BALF was obtained by injecting and withdrawing phosphate-buffered saline (PBS) 3 times at 4, 3 and 3ml volumes to reach a final amount of 10ml for each animal. After lavage, lungs were removed from the chest

and separated from extrapulmonary structures, then stored at -20 degrees Celsius for further studies.

2.2.3 Analysis of BALF

Total leukocyte counts were determined using a hemocytometer (Hausser Scientific ,Horsham, PA) at a magnification of 400x. The BALF was then centrifuged for 3 minutes at 5 shelves, the supernatant was removed and stored at -20 degrees Celsius for further analysis. Differential cell counts were performed by resuspension of the pellet in 1ml PBS, followed by plating of the cells onto microscopic slides with a cytocentrifuge (Shandon Inc., Pittsburgh, USA) for 5 minutes at a speed of 1000 rpm. The slides were air dried, fixed in methanol for 5-7 minutes, treated with Giemsa stain, and coverslipped using Cytoseal. At least 200 cells were identified using standard morphological criteria to determine percent neutrophil in BALF.

2.2.4 Histological evaluation of lungs

After euthanasia, the lungs were fixed with 10% neutral-buffered formalin for 2 hours at a pressure of 20 cm H_2O, then removed from the chest and immersed in formalin for 48 hours. Following removal of extrapulmonary structures, the samples were cut into random pieces and placed in cassettes for histological processing. The cassettes were passed through graded concentrations of ethanol, ranging from 35% to 100%, for 5 minute intervals, followed by repeated immersion in clean 100% xylene for 15, 25 and 40 minutes. The samples were

then sequentially incubated in xylene-paraffin mixture (1:1) for 1 hour, 100% paraffin for 1 hour and fresh 100% paraffin for 2 hours. They were finally embedded in blocks of paraffin wax, using a Leica 1160 tissue-embedding machine. The resulting tissue blocks were stored in a refrigerator prior to processing with a microtome. Tissue sections (5µm thickness) were cut with a standard rotary microtome (American Optical Company), floated in a water bath at 55 degrees Celsius, then layered on Vectabond™ coated slides, and incubated at 55 degrees Celsius overnight for future studies.

2.2.5 Hemotoxylin and Eosin Staining (H&E)

Tissue sections were deparaffinized in three changes of xylene for 5 minutes each, then rehydrated in graded concentrations of ethyl alcohol(ETOH) (100%, 95%, 70%, 30%) for 2 minute intervals, followed by washing in distilled water for 1 minute. The sections were then stained with hematoxylin for 10 minutes, and sequentially immersed in distilled water for 2 minutes, ammonium chloride (NH4CL) and ETOH for 1 minute, tap and distilled water for 1 minute each, and 70% ETOH for 2 minutes. The sections were then counterstained in eosin solution for 2 minutes and then dehydrated in alcohol as follows: 95% ETOH for 2 minutes and 3 changes of 100% ETOH for 2 minutes each. Finally, sections were cleared in 3 changes of xylene 2 minutes each mounting with coverslips using permount.

2.2.6 Verhoeff's Elastic Fiber Stain (VEG)

Slide sections were deparaffinized in three changes of xylene for 5 minutes each, then rehydrated in distilled water for 1 minute. They were then stained in Verhoeff's solution for 30 minutes. They were rinsed in 3 changes of tap water and differentiated in 2% ferric chloride solution for 2 minutes. At this step, black elastic fibers were observed microscopically on a grey background. The differentiation was stopped by washing the slides in a 2-3 changes of tap water. They were then treated in 5% sodium thiosulfate for 1 minute and washed in running tap water for 5 minutes. They were then counterstained in Van Gieson's solution for 5 minutes, dehydrated quickly through 95% alcohol and 2 changes of 100% alcohol, and cleared in 2 changes of xylene for 3 minutes each. Finally, they were coverslipped with mounting medium.

2.2.7 Microscopic Studies

The slides' labels were covered and named randomly to avoid bias. The slides were then evaluated under light microscopy at 100x magnification with American Optics microscope. Photomicrographs of the slides were taken using Amscope MU1003 camera and ToupLite software to determine the percent surface area of both the lung and interstitial elastic fibers with ImageJ software. For each specimen, a minimum of 25 photomicrographs were captured and the results were demonstrated as the mean percentage of surface area at 100x magnification. Microscopic fields containing prominent blood vessels or airways were not included in the analyses.

Additionally, MLI was determined using a standard test grid over lung photomicrographs to count the number of intersections of alveolar walls with grid lines (50,51). Areas of hyperinflation or inadequate inflation were excluded. ISA per unit lung volume was measured using MLI values (52).

2.2.8 Measurement of BALF DID

Free and total BALF DID levels were measured using a combination of liquid chromatography and tandem mass spectrometry (LC/MS/MS). To measure free BALF DID levels, the supernatants previously collected and stored were concentrated to 0.5 ml and combined with 10% trifluoro-acetic acid to precipitate proteins. Following centrifugation, the samples were mixed with butanol, glacial acetic acid and water (4:1:1), then applied to a CF1 column, washed and eluted. For measuring total BALF DID levels, 2 ml of supernatants were mixed with an equal volume of 37% HCL and hydrolyzed at 110 degrees Celsius for 24 hour. The samples were then dried under vacuum, combined with 2 ml of butanol, glacial acetic acid and water (4:1:1), applied to a CF1 column, washed and eluted. Separation of the crosslinks was performed with a 2 × 100 mm dC18 column (Water Corporations, Milford, MA), using a combination of mobile phases: (A) 7 mM heptafluorobutyric acid (HFBA) and 5 mM ammonium acetate in water, and B) 7 mM HFBA and 5 mM ammonium acetate in 80% acetonitrile. The BALF samples which had been filtered and dried following CF1 chromatography, were dissolved in mobile phase A and applied to the column. The elution gradient was performed linearly from 100 to 90% A over a 10-minute interval, and the

separated crosslinks were analyzed with a TSQ Discovery electrospray tandem mass spectrometer (Thermo Fisher Scientific, Waltham, MA), using selected reaction monitoring of mass to charge ratio transitions. The results were quantified by comparison with a d4-labeled desmosine standard.

2.2.9 Measurement of Lung DID

Whole lungs, free of extrapulmonary structures were washed to remove blood. They were then homogenized by ultrasonication and centrifuged. The supernatant was decanted and the pellet was resuspended in PBS and again centrifuged. This process was repeated twice and the remaining tissue was hydrolyzed in 37% HCL at 110 degrees Celsius for 24 hours. Total lung DID levels were then determined following the steps described above.

2.2.10 Chemotaxis Assay

BALF leukocytes from untreated animals were centrifuged and suspended in Dulbecco's culture medium. They were gently mixed to ensure uniformity and placed in the upper wells of Boyden chambers with a 3 µm pore size membrane (Sigma-Aldrich, ST Louis, MO) and exposed to either: 1) 100 µg of elastin peptides and 10 µg LPS 2) 100 µg elastin peptides alone 3) 10 µg LPS alone, or 4) neither elastin peptides nor LPS (controls) in the lower wells. The lower wells were filled with additional media to cover base of the upper wells. The same volume of media was used for each well. Additional chambers only contained culture medium in both upper and lower wells and were used for background

measurements. Following incubation at 37 degrees Celsius for 24 hours, cells were carefully removed from the top side of the insert. The contents of the lower wells were gently mixed to evenly distribute the cells. Cell migration through the membrane was determined with a CyQuant® cell assay kit (Thermo Fisher, Waltham, MA) which uses a fluorescent dye that binds to DNA. The treated cells were transferred to a 96-well microplate and a combination of fluorescent dye solution and lysis buffer was added to each well. The samples were incubated at room temperature for 15 minutes and fluorescence emission was measured with a fluorescent plate reader using a 480/520 nm filter set.

2.2.11 Detection and quantification of apoptotic cells by terminal deoxynucleotide transferase mediated dUTP nick end labeling (TUNEL) assay

The focal in situ apoptosis at the level of the pulmonary alveolar epithelium was determined using a terminal deoxynucleotide transferase mediated dUTP nick end labeling (TUNEL) kit (Chemicon International Inc, USA) on the paraffin-embedded sections of the lung samples according to the manufacturer's protocol. The slides were deparaffinized in xylene three times for 5 minutes each, followed by rinsing in 2 changes of 100% ETOH for 5 minutes each, one change of 95% and one change of 70% ETOH for 3 minutes each, and in one change of PBS for 5 minutes. They were then incubated in proteinase K (20 µg/mL) for 15 minutes at room temperature in a coplin jar. After washing the samples twice with distilled water for 2 minutes each, the slides were quenched with 3% hydrogen peroxide in

PBS for 5 minutes at room temperature, again washed twice with PBS for 5 minutes each. The excess liquid on the slides was blotted and 75 µL/5cm^2 of equilibration buffer was directly applied on the slides for 30 seconds. The excess liquid on the sample slides was blotted and this time 55 µL/5cm^2 of working strength TdT enzyme was added to the slides and incubated in a humified chamber at 37 degrees Celsius for 1 hour.

The reaction was then terminated by application of stop buffer, being agitated for 15 seconds followed by incubation at room temperature for 10 minutes. The specimens were then washed in three changes of PBS for 1 minute each. After blotting the excess liquid, 65 µL/5 cm^2 of room temperature anti-digoxigenin conjugate was applied directly on the slides and incubated in a humidified chamber for 30 minutes at room temperature. The slides were then washed in four changes of PBS for 2 minutes each. After blotting the excess liquid, 75 µL/5 cm^2 of peroxidase substrate was applied to cover the entire slide. They were then stained for 6 minutes at room temperature.

After staining, the specimens were washed in 3 changes of distilled water for 1 minute each and incubated in distilled water in a coplin jar for 5 minutes at room temperature. The slides were then counterstained in 0.5% methyl green for 10 minutes at room temperature, washed in three changes of distilled water in a coplin jar, dipping the slides 10 times each in the first and second washes, followed by 30 seconds without agitation in the third wash. The slides were then washed in three changes of 100% n-butanol in a coplin jar following the same protocol as distilled water. The specimens were then dehydrated by using three

changes of xylene for 2 minutes each and mounted with coverslip using permount.

TUNEL positive apoptotic cells were identified as brown stained cells under 400x magnification. The number of TUNEL positive cells in 20 fields was counted for each sample.

2.2.12 Statistical Analysis

One-way analysis of variance (ANOVA) and Bonferroni post-hoc test were used to determine statistically significant differences among treatment groups. A p-value of less than 0.05 was considered statistically significant. Results were expressed as mean ± standard error of mean (SEM).

Chapter 3: Results

3.1 BALF Total Leukocyte Count

Bronchoalveolar lavage was performed 48 hours after LPS administration. Animals treated with elastase/LPS had a significant increase in the number of BALF leukocytes (187×10^4) compared to elastase alone (37.3×10^4; $p<0.0001$), LPS alone (23.0×10^4; $p<0.0001$), or controls (47.7×10^4; $p<0.0001$) (Figure 1).

3.2 Percent BALF Neutrophils

BALF neutrophils were significantly increased in the elastase/LPS group (39 percent) compared to the elastase alone (3.4 percent; $p<0.0001$), LPS alone (14 percent, $p<0.0001$), or controls (4.8 percent; $p<0.0001$) (Figure 2).

3.3 Lung Surface Area Measurements

Determination of mean percent surface area of the lungs was performed 7 days post-LPS treatment. Animals receiving elastase/LPS had a significantly decreased percentage surface area compared to controls receiving saline alone (17.8 vs 25.5 percent; $p<0.0001$). Those given elastase or LPS alone also had a significant

decrease in the percent surface area compared to controls (19.7 percent and 20.1 percent, respectively, p,0.001), however this reduction was less prominent compared to the elastase/LPS group (Figure 3 and 4).

3.4 Elastic Fiber Surface Area

Measurements of elastic fiber surface area (as a percentage of total surface area) were made 7 days after LPS-treatment. Elastic fiber surface area was significantly increased in the elastase/LPS group compared to LPS only and controls (49 vs 40 and 26 percent, respectively). Elastase and LPS only groups also showed a significant elevation in elastic fiber surface area compared to controls (45 and 40 vs 26 percent, respectively) (Figure 5).

Animals treated with elastase/LPS showed more prominent splaying and fragmentation of lung elastic fibers due to increased lung elastin degradation. Less noticeable but similar changes were observed in the LPS and elastase only groups. The increase in the elastic fiber surface area can partly be explained by the structural alterations in elastic fibers (Figure 6).

3.5 Mean Linear Intercept and Internal Surface Area

Measurements of MLI and ISA was performed 7 days post-LPS treatment. Animals treated with elastase/LPS showed a significant increase in MLI (156.2 μm; $p<0.0001$) compared to those receiving LPS (98.0), elastase (85.5), and

controls (81.7). Additionally, the elastase/LPS group showed a significant decrease in ISA (25.7 mm^2 per mm^3 lung volume; $p<0.0001$) compared to the LPS group (40.9), elastase group (46.8), and controls (49.4) (Figure 7 and Table 1).

3.6 Total and Free BALF DID

Measurements of free and total BALF DID levels were performed 48 hours post-LPS treatment. Free BALF DID levels were significantly higher in the elastase/LPS group compared to the elastase only group (182 vs 97 percent of control; $p<0.05$), however, the LPS only group did not show a significant difference from the elastase only group (Figure 8).

Higher levels of total BALF DID was also noticed in the elastase/LPS group compared to the LPS and elastase only groups with no statistical significance (Figure 9). Previous studies in our laboratory have also identified free DID levels as a more sensitive biomarker of elastic fiber degeneration compared to total DID (53).

3.7 Total Lung DID

Measurements of total lung DID were made 48hours post- LPS treatment. Animals treated with elastase/ LPS or elastase only demonstrated an increase in

total lung DID levels compared to controls although not significant (288 and 312 vs 243 ng/mg dry lung) (Figure 10).

3.8 Effects of Exogenous Elastin Peptides on BALF Cell Count and BALF DID

Lungs treated with LPS and elastin peptides showed a significant increase in percentage of BALF neutrophils compared to those treated with LPS or peptides alone (37 vs 10 and 1.2 percent, respectively; $p<0.0001$) (Figure 12). However, total BALF leukocyte values were not significantly different between the groups (Figure 11).

Measurements of free and total BALF DID were made 48 hours after LPS and/or elastin peptides treatment. Animals treated with both LPS and peptides had a significant increase in free BALF DID levels (as a percentage of control) compared to those given peptides alone and controls (330 vs 133 percent; $p<0.05$ and 330 vs 100; $p<0.01$). However, there was no statistical significance between the LPS and peptide only groups (Figure 13).

Total BALF DID levels were also increased in animals treated with LPS and elastin peptides with no statistical significance compared to other groups (Figure 14).

3.9 Chemotaxis Assay

The chemotactic activity of BALF leukocytes was determined in animals treated with LPS and elastin peptides, peptides alone, LPS alone and controls. Differential cell counts consisted of 98 ± 1.5 percent macrophages in the LPS and peptide group. Chemotaxis was significantly increased in animals treated with peptides alone and LPS alone compared to controls (145 and 109 vs 12 relative fluorescence units $\times 10^4$ cells, respectively). However, treatment with LPS and elastin peptides resulted in a much greater chemotactic activity compared to controls or either agent alone (230 units $\times 10^4$ cells) (Figure 15).

3.10 TUNEL Assay

Apoptosis of lung cells was measured in lung samples of the elastase/LPS, elastase only and control groups. TUNEL positive cells were significantly higher in the elastase/LPS group compared to both elastase and control groups (13.28 vs 4.88 and 3.20 per HPF; $p<0.0001$) (Figure 16).

Chapter 4 : DISCUSSION

4.1 COPD Exacerbations

COPD exacerbations are defined as acute worsening of symptoms, including dyspnea, cough, sputum production and purulence (54). Exacerbation episodes are very common and the most important risk factor is previous history of exacerbations (55). Acute exacerbations are known to accelerate the progressive decline in lung function which is the main characteristic of COPD (56). The vast majority of COPD exacerbations are induced by bacterial or viral respiratory infections with non-typeable Hemophilus Influenzae considered the most prevalent pathogen (13). Additionally, around 30% of exacerbations are caused by environmental pollution or unknown etiologies (13). The presence of other comorbidities, especially congestive heart failure and pneumonia not only further complicates exacerbations but also makes it more difficult to determine the cause of the symptoms (13).

4.2 Management of COPD Exacerbations

The major goal of management of COPD exacerbations is to reduce the severity and frequency of exacerbation episodes (21). The most common pharmacological treatments used for exacerbations are corticosteroids, bronchodilators, and antibiotics. Systemic corticosteroids have been long used for treating exacerbations of COPD due to their anti-inflammatory effects (12). However,

their use in the treatment of exacerbations has been controversial as they have sometimes failed to treat acute and severe episodes of exacerbations (57). Additionally, corticosteroids have been a less desirable option for treatment of stable COPD due to their adverse effects and high costs (21). Bronchodilators are the most common pharmacological treatment used in COPD which include short- and long-acting β2 agonists, anticholinergic antimuscarinic agents, and theophylline . Short-acting β2 agonists such as albuterol and antimuscarinic agents like ipratropium bromide are most commonly used during exacerbations. On the other hand, long-acting β2 agonists such as salmeterol are mostly used for treatment of stable COPD (13). Theophylline is a methylxanthine which has both bronchodilatory and anti-inflammatory effects but its use in early treatment of exacerbations is questionable due to many serious side effects and limited efficacy in improving lung function (58).

The prophylactic use of antibiotics for COPD exacerbations has also been controversial as MacNee et al. proved them to be ineffective in reducing the frequency of episodes (59). On the other hand, Ko et al. stated that prophylactic use of antibiotics, especially macrolides has proved to decrease the frequency of COPD exacerbations due to the more prevalent infectious etiology of exacerbations(12).

4.3 Effect of Lung Remodeling on progression of COPD

The biomechanics and interplay between the components of lung tissue and ECM are of significant importance in lung parenchymal injuries and subsequent tissue repair (60,61). Lung repair and remodeling processes further deteriorate airspace enlargement and airway obstruction, as prominent hallmarks of emphysema, due to disruption in mechanical forces, and loss of elastic recoil causing greater strain on alveolar walls (62,63). This rise in airspace pressure contributes to more prevalent alveolar destruction and rupture as elastic fiber degradation progresses (64). Additionally, there is some evidence that impaired resynthesis of elastin may play a major role in the pathogenesis of COPD. Although elastic fiber regeneration can partially restore the elastin content of airspaces, it does not reconstruct the complicated biostructure of the lungs leading to reduced lung function (65).

4.4 Inflammatory Cells and Exacerbations

Inflammation is regarded as a major characteristic of COPD with an increased level of neutrophils, lymphocytes and eosinophils detected in the lungs during exacerbations (66). Neutrophil elastase and myeloperoxidase enhance the inflammatory response in the lungs during exacerbations, induce oxidative stress and damage the important crosslinks in the ECM of the lungs. Although anti-inflammatory agents have been used in the treatment of COPD exacerbations, it is

important to investigate therapies that specifically target neutrophil recruitment and activation, and could potentially inhibit release of neutrophil elastase (67). Therefore, further studies are required to fully understand the inflammatory pathways involved in exacerbations to develop more effective treatment strategies for COPD exacerbations.

4.5 DID Crosslinks in COPD

DID crosslinks are an integral part of elastic fibers and their level in body fluids, including blood, sputum or urine can determine the progression and severity of COPD (68,69). The level of these lysyl-derived tetrafunctional amino acids in blood or sputum may be useful in assessing the efficacy of treatment in COPD as they reflect elastic fiber turnover in emphysema (32,70).

Significantly increased levels of free BALF DID in animals treated with both elastase and LPS suggest that superimposed inflammation accelerates degradation of structurally altered elastic fibers in COPD exacerbations. This is consistent with enhanced splaying and fragmentation of elastic fibers observed in the elastase/LPS group in this study. The unraveling of these fibers make them more susceptible to enzymatic and oxidative breakdown by either loss of DID crosslinks or defective repair mechanisms to regenerate them, leading to further airspace enlargement and rupture. This phenomenon can contribute to the progressive decline in lung function known to occur during COPD exacerbations.

Upregulation of elastin resynthesis after breakdown of DID crosslinks may be helpful in treating COPD exacerbations or reducing their frequency. Joddar et al. showed that vascular smooth muscle cells can exhibit elastogenic effects when exposed to hyaluronan (HA) oligomers (71).

Total lung DID content was not elevated in the elastase/LPS group in contrast to free BALF DID. This is consistent with findings of Deslee et al. who demonstrated no increase in lung desmosine content in severe COPD despite a significant increase in elastic fiber surface area as a percentage of total lung tissue (72).

4.6 Percent Lung and Elastic Fiber Surface Area

Our results demonstrated that percent lung surface area was significantly decreased in the elastase/LPS group. This signifies the widespread lung parenchymal destruction during COPD exacerbations which occurs as a result of the complicated and yet not fully known pathophysiology of the disease. Regeneration and repair of the lung alveoli may be beneficial in preventing further lung destruction in exacerbations. The possible role of stem cell therapy in COPD to restore the intricate architecture of lung airspaces has been an interesting topic with clinical trials reporting minimal to no improvement in lung function after administration of these cells (73). Additional larger scale clinical

trials are needed to further explore this potential advanced treatment approach for COPD and exacerbations.

Deslee et al. showed that elastin expression is considerably elevated in stage 4 COPD indicating the potential role of an enhanced alveolar repair mechanism in very severe COPD (72). Introducing cells that either replace the lost pneumocytes in COPD, or proliferate and differentiate into the damaged tissue could represent a major advancement in the treatment of COPD exacerbations through alveolar regeneration (74). As current therapies for COPD exacerbations are palliative and the only permanent treatment strategy to prevent further lung deterioration is transplantation, further studies should investigate the potential benefits of regenerative therapy in COPD.

4.7 Elastin Peptides and Exacerbations

We determined that elastin peptides as products of elastic fiber breakdown act as chemo-attractants for inflammatory cells causing an influx of neutrophils into the lungs in response to LPS. This indicates that the more prominent and progressive structural and functional lung deterioration during COPD exacerbations is due to an enhanced level of elastin peptides in the alveoli. These findings are consistent with in vitro studies showing elastin fragments to intensify the inflammatory response in emphysema by attracting leukocytes into the lungs (75,76). Additionally, intratracheal instillations of EP in mice resulted in emphysematous

changes as well as inflammatory cell accumulation in the lungs (77). Another study found that despite smoking cessation, the number of inflammatory cells in airspaces remained the same (78). This persistent inflammation in COPD and specifically emphysema has been described as an autoimmune-mediated process supporting the theory that COPD mimics autoimmune disorders (79). As a result, COPD exacerbations may resemble the flare-ups experienced in autoimmune diseases enhancing elastolysis. This is an interesting area for future research to investigate the use of immunosuppressive drugs for COPD exacerbations.

The significant elevation in BALF DID levels in LPS/peptides group suggests the important role of these fibers in the prognosis of exacerbations. Introducing agents that can either inhibit elastic fiber breakdown or remove elastin peptides may prevent the progressive decline in lung function during exacerbations. For instance, aerosolized HA has shown to decrease airspace enlargement in emphysema by preferentially binding to elastic fibers in both in vitro and vivo models (80,81). In a pilot clinical trial, plasma and sputum levels of DID were substantially reduced in COPD patients who used aerosolized HA for a 3-week period (82). Further studies are required to explore other potential pharmacological agents to prevent elastic fiber degeneration or remove elastin peptides in COPD exacerbations.

4.8 Role of Chemotaxis in Exacerbations

Our results indicated a significant increase in the chemotactic activity of leukocytes in vitro when exposed to LPS/peptides compared to all other groups. Increased chemotaxis of leukocytes has previously been reported in COPD patients (43,44,83) .These findings are crucial in understanding the pathogenesis of COPD exacerbations as they support the theory that elastic fiber breakdown products display pro-inflammatory effects in the course of exacerbations which could enhance the influx of inflammatory cells, especially neutrophils into the lungs. This elevated inflammatory response will accelerate lung destruction and airspace enlargement which are characteristic of exacerbations. Therefore, the potential effect of chemotaxis antagonists like LTB4 inhibitors should be investigated in prevention and treatment of COPD exacerbations through reduction of chemotactic activity of neutrophils.

4.9 Role of Apoptosis in Exacerbations

Our results demonstrated a significant increase in the number of apoptotic cells in the elastase/LPS group. Increased apoptosis in the lungs of COPD patients was first reported in a study by Segura-Valdez et al. in which they showed a significant elevation in endothelial and epithelial cell death in lung tissues of COPD patients (46). Additionally, Markis et al. detected a significant increase in the number of apoptotic neutrophils in COPD patients which may had been

caused by either an impairment in the apoptotic mechanisms or decreased clearance of apoptotic cells from the lungs (49).Therefore, different apoptotic pathways are activated in COPD patients which explains the progressive deterioration in lung function even after smoking cessation (84). Furthermore, an imbalance between pro- and anti-apoptotic factors was indicated in COPD patients supporting the role of apoptosis in the intricated pathogenesis of the disease. As a result, restoring this imbalance and inhibiting apoptosis in the lungs during exacerbations can be a novel therapeutic strategy for COPD exacerbations.

4.10 Conclusions

Structural alterations in elastic fibers during exacerbations make them more susceptible to degradation and enhance the release of pro-inflammatory cells. Elastic fiber breakdown products (elastin peptides) further augment the inflammatory response in the lungs. These mechanisms result in increased alveolar destruction and airspace enlargement which further enhances the progression of the disease. Understanding the pathogenesis of COPD exacerbations and the complex interplay between different mechanisms, including protease-antiprotease imbalance, apoptosis, oxidative stress, and the pro-inflammatory effect of elastin peptides, may lead to more effective approaches to the treatment of this condition.

Table 1

Mean Linear Intercept and Internal Surface Area

Group	**Control**	**Elastase**	**LPS**	**Elastase + LPS**
N	8	4	4	4
Mean Linear Intercept (μm)	81.7 ± 2.9	85.5 ± 1.0	98.0[a] ± 2.1	156.2[b] ± 4.9
Internal Surface Area (mm^2 per mm^3 volume)	49.4 ± 1.8	46.8 ± 0.6	40.9[c] ± 0.9	25.7[b] ± 0.8

Table showing mean linear intercept and internal surface area values. Results were expressed as mean ± SEM. Comparison among groups was done using one-way ANOVA followed by Bonferroni multiple comparison post-hoc test.

(a: $p<0.05$ vs control; b: $p<0.0001$ vs all other groups; c: $p<0.01$ vs control

Figure 1

Total BALF Leukocyte Counts

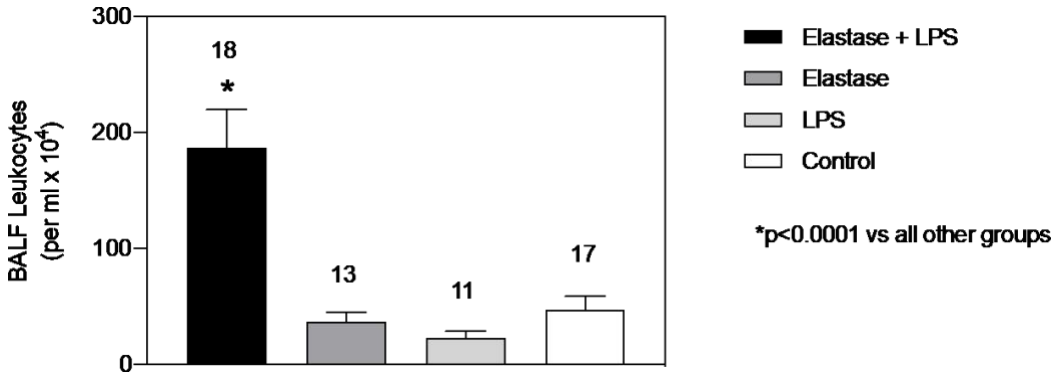

Graph showing the total BALF leukocyte counts. The animals were treated with either IT elastase/LPS, elastase, LPS, or NS (control). The animals were euthanized 48 hours after IT treatment. Results were expressed as mean ± SEM. Comparison among groups was done using one-way ANOVA followed by Bonferroni multiple comparison post-hoc test.

Figure 2

Percent BALF Neutrophil Content

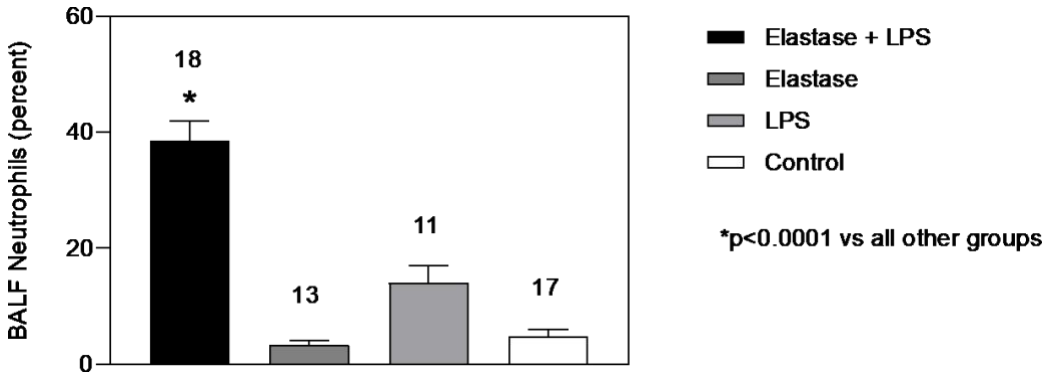

Graph showing the percent BALF neutrophil content. The animals were treated with either IT elastase/LPS, elastase, LPS, or NS (control). The animals were euthanized 48 hours after IT treatment. Results were expressed as mean ± SEM. Comparison among groups was done using one-way ANOVA followed by Bonferroni multiple comparison post-hoc test.

Figure 3

Percent Lung Surface Area

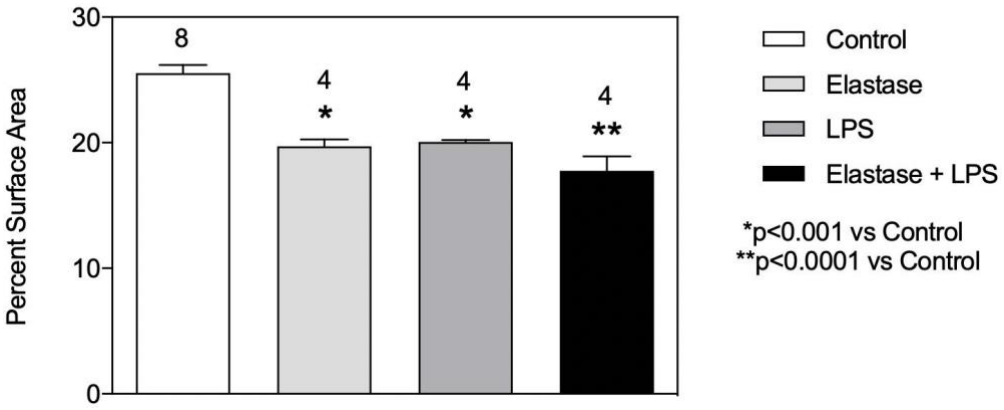

Graph showing the percent lung surface area. The animals were treated with either IT elastase/LPS, elastase, LPS, or NS (control). The animals were euthanized 7 days after IT treatment. Results were expressed as mean ± SEM. Comparison among groups was done using one-way ANOVA followed by Bonferroni multiple comparison post-hoc test.

Figure 4

Hemotoxylin and eosin staining of paraffin sections of the lungs

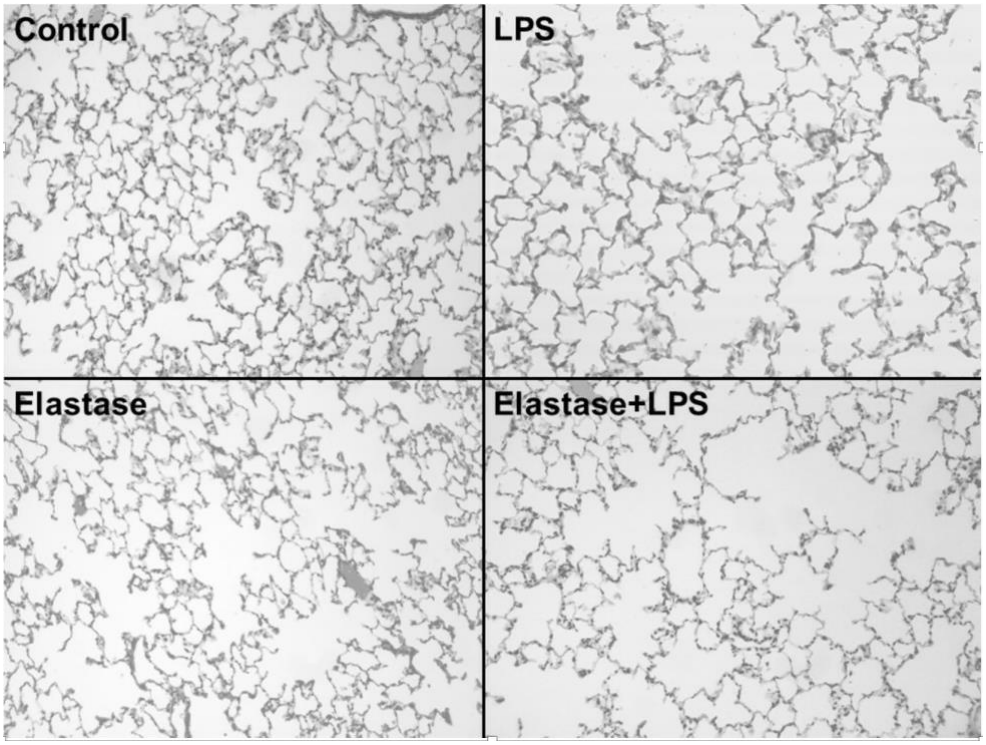

Photomicrograph of paraffin sections from hamster lungs stained with hemotoxylin and eosin. Upper left photomicrograph represents the lung of an animal treated with IT NS. The upper right photomicrograph represents the lung of an animal treated with IT LPS. The lower left photomicrograph represents the lung of an animal treated with IT elastase. The lower right photomicrograph represents the lung of an animal treated with IT elastase/LPS. The animals were euthanized 7 days after IT treatment. Measurement were taken at magnification of 100x.

Figure 5

Percent Interstitial Elastic Fiber Surface Area

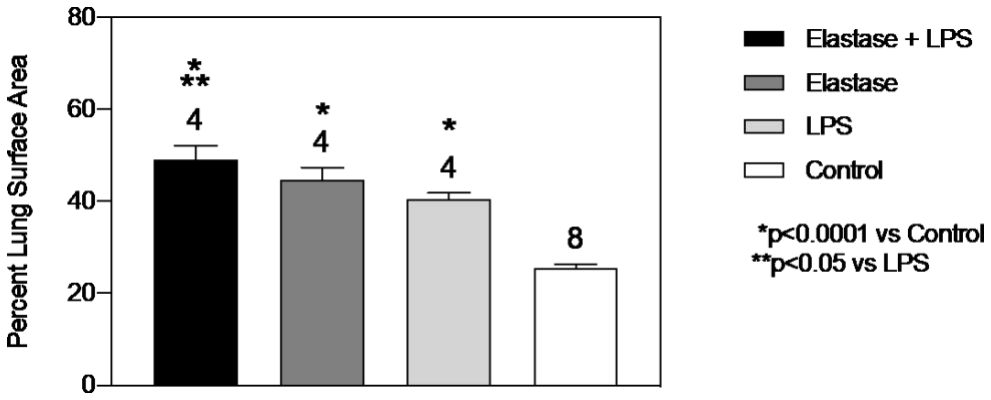

Graph showing the percent interstitial elastic surface area. The animals were treated with either IT elastase/LPS, elastase, LPS, or NS (control). The animals were euthanized 7 days after IT treatment. Results were expressed as mean ± SEM. Comparison among groups was done using one-way ANOVA followed by Bonferroni multiple comparison post-hoc test.

Figure 6

Verhoeff's Staining of Lung Elastic Fibers

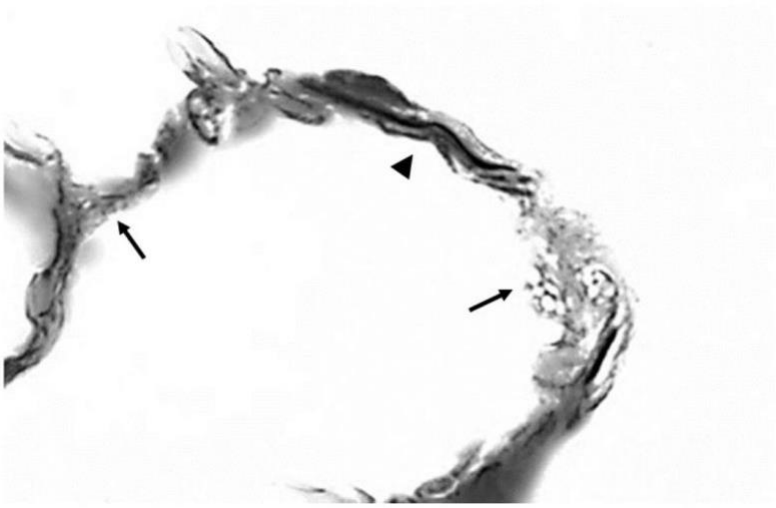

Photomicrograph of elastic fiber of the lung of an animal treated with elastase/LPS showing areas of structural alterations in elastic fibers, including splaying (arrowhead) and fragmentation (arrows).

Figure 7

Mean Linear Intercept

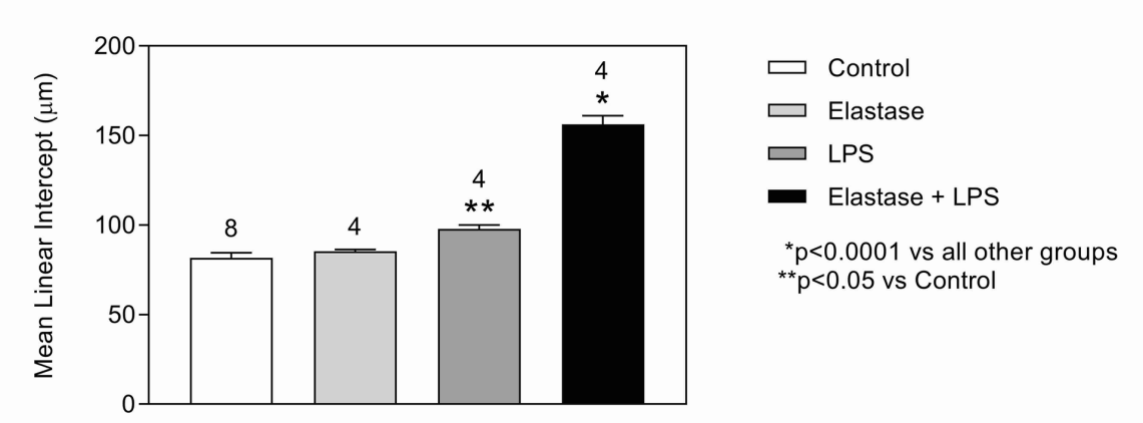

Graph showing mean linear intercept values. The animals were treated with either IT elastase/LPS, LPS, elastase, or NS (control). The animals were euthanized 7 days after IT treatment. Results were expressed as mean ± SEM. Comparison among groups was done using one-way ANOVA followed by Bonferroni multiple comparison post-hoc test.

Figure 8

Free BALF DID Content

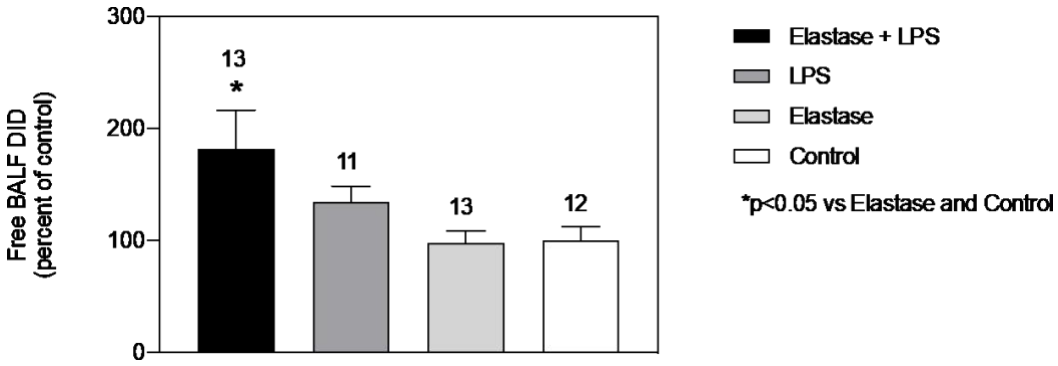

Graph showing the free BALF DID content. The animals were treated with either IT elastase/LPS, LPS, elastase, or NS (control). The animals were euthanized 48 hours after IT treatment. Results were expressed as mean ± SEM. Comparison among groups was done using one-way ANOVA followed by Bonferroni multiple comparison post-hoc test.

Figure 9

Total BALF DID Content

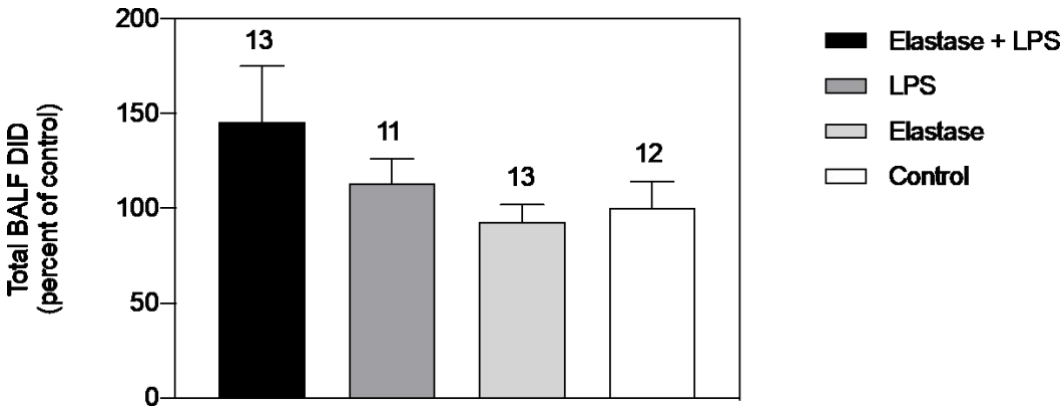

Graph showing the total BALF DID content. The animals were treated with either IT elastase/LPS, LPS, elastase, or NS (control). The animals were euthanized 48 hours after IT treatment. Results were expressed as mean ± SEM. Comparison among groups was done using one-way ANOVA followed by Bonferroni multiple comparison post-hoc test.

Figure 10

Total Lung DID Content

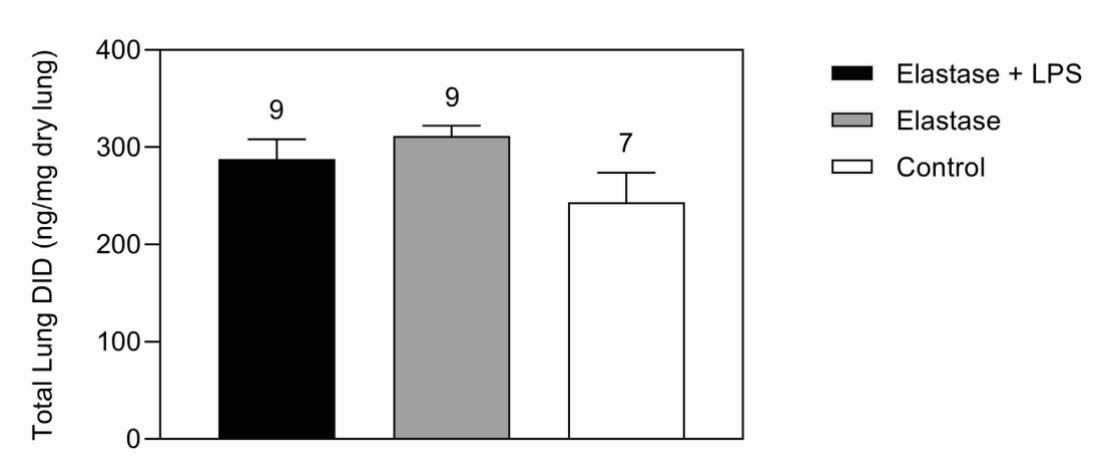

Graph showing the total lung DID content. The animals were treated with either IT elastase/LPS, elastase, or NS (control). The animals were euthanized 48 hours after IT treatment. Results were expressed as mean ± SEM. Comparison among groups was done using one-way ANOVA followed by Bonferroni multiple comparison post-hoc test.

Figure 11

Total BALF Leukocyte Counts

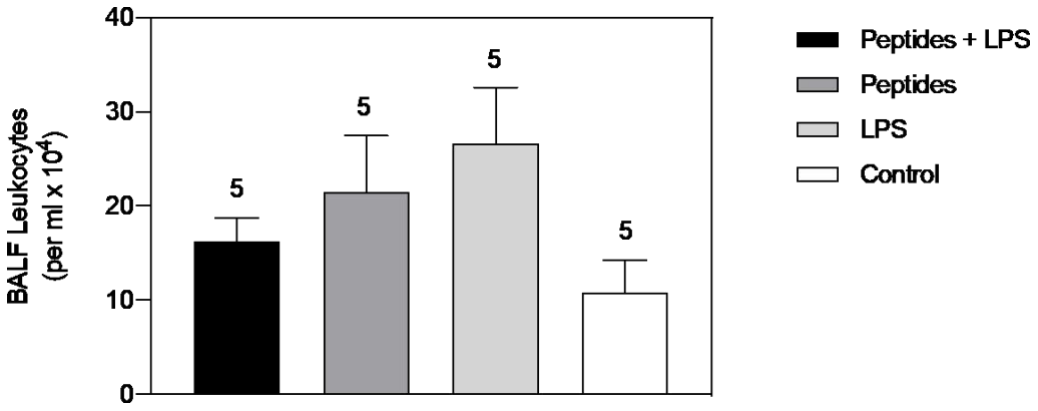

Graph showing the total BALF leukocyte counts. The animals were treated with either IT peptides/LPS, peptides, LPS, or NS (control). The animals were euthanized 48 hours after IT treatment. Results were expressed as mean ± SEM. Comparison among groups was done using one-way ANOVA followed by Bonferroni multiple comparison post-hoc test.

Figure 12

Percent BALF Neutrophil Content

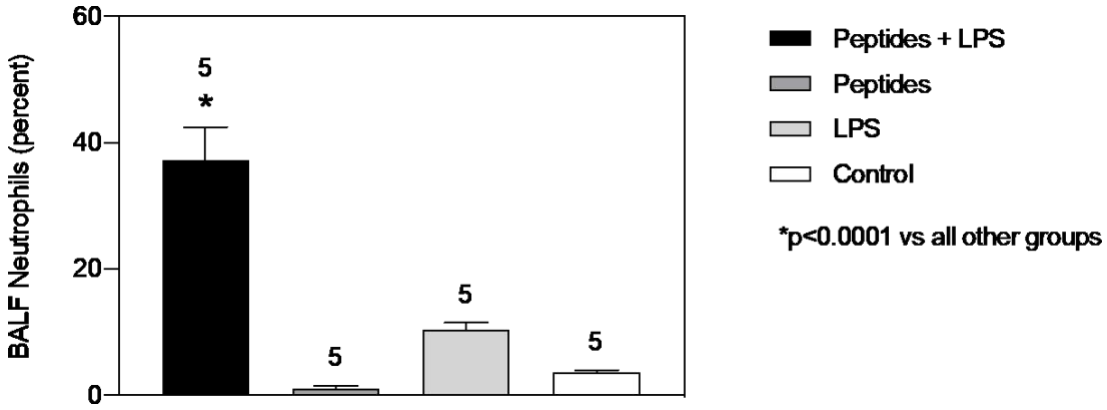

Graph showing the percent BALF neutrophil content. The animals were treated with either IT peptides/LPS, peptides, LPS, or NS (control). The animals were euthanized 48 hours after IT treatment. Results were expressed as mean ± SEM. Comparison among groups was done using one-way ANOVA followed by Bonferroni multiple comparison post-hoc test.

Figure 13

Free BALF DID Content

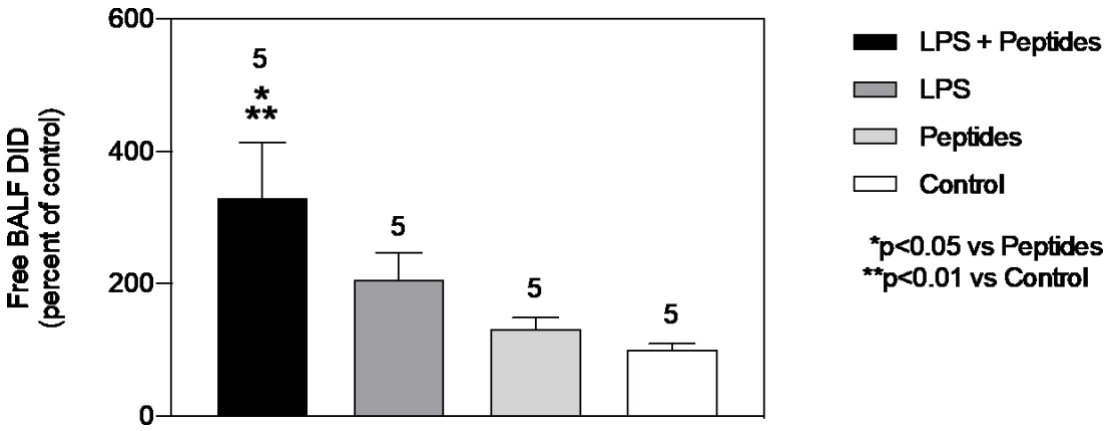

Graph showing the free BALF DID content. The animals were treated with either IT peptides/LPS, LPS, peptides, or NS (control). The animals were euthanized 48 hours after IT treatment. Results were expressed as mean ± SEM. Comparison among groups was done using one-way ANOVA followed by Bonferroni multiple comparison post-hoc test.

Figure 14

Total BALF DID Content

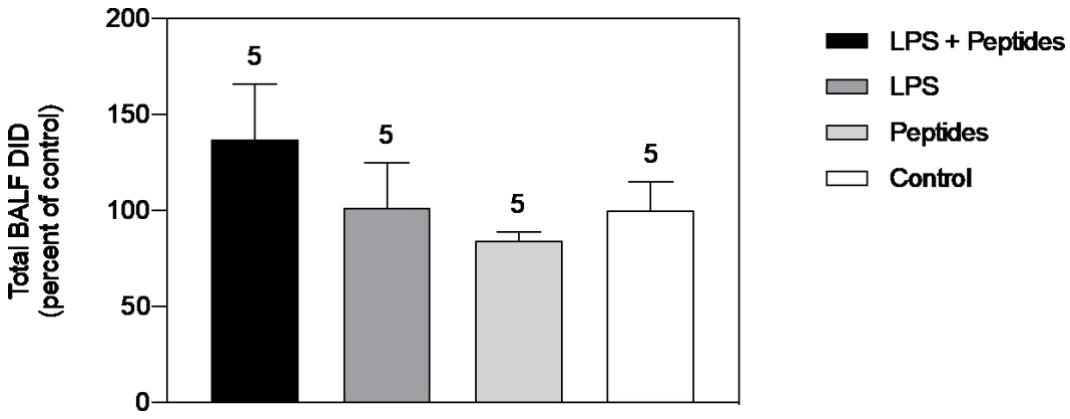

Graph showing the total BALF DID content. The animals were treated with either IT peptides/LPS, LPS, peptides, or NS (control). The animals were euthanized 48 hours after IT treatment. Results were expressed as mean ± SEM. Comparison among groups was done using one-way ANOVA followed by Bonferroni multiple comparison post-hoc test.

Figure 15

Chemotaxis Assay

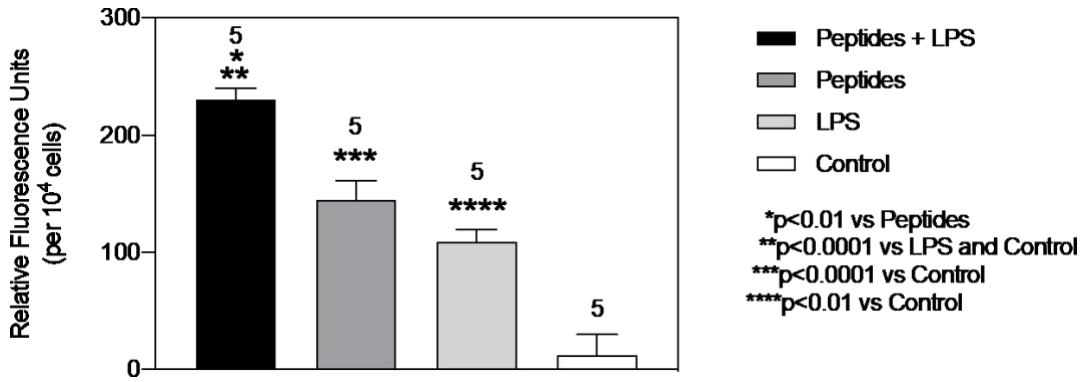

Graph showing chemotaxis assay results. BALF leukocytes from untreated animals were exposed to either peptides/LPS, peptides, LPS, or NS (control) in a Boyden chamber (chemotaxis) assay. Relative fluorescence emission of leukocytes were measured at a fluorescent plate reader using a 480/520 nm filter set. Results were expressed as mean ± SEM. Comparison among groups was done using one-way ANOVA followed by Bonferroni multiple comparison post-hoc test.

Figure 16

TUNEL Assay

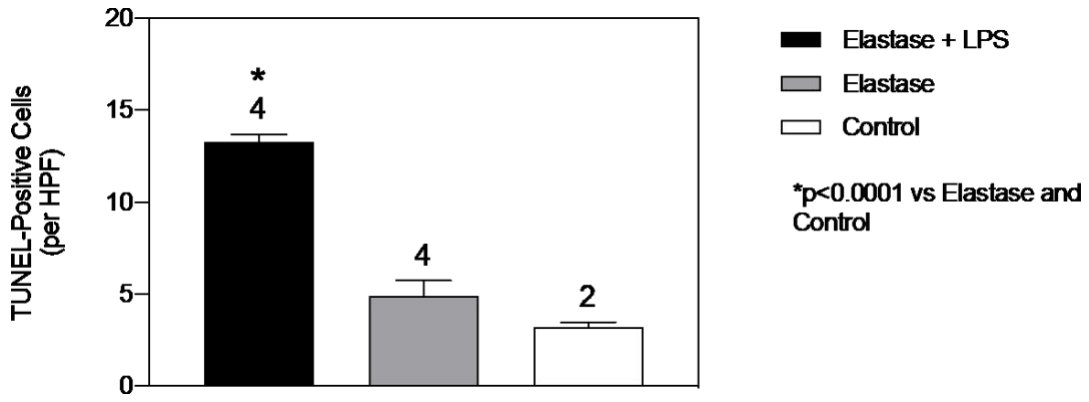

Graph showing TUNEL assay results. Paraffin sections of the lungs of animals treated with either IT elastase/LPS, elastase, or NS (control) were evaluated to detect and quantify apoptotic cells by terminal deoxynucleotide transferase mediated dUTP nick end labeling (TUNEL) assay. Number of brown-stained apoptotic cells were counted at magnification of 400x. Results were expressed as mean ± SEM. Comparison among groups was done using one-way ANOVA followed by Bonferroni multiple comparison post-hoc test.

References

1. Fischer BM, Pavlisko E, Voynow JA. Pathogenic triad in COPD: Oxidative stress, protease-antiprotease imbalance, and inflammation. Vol. 6, International Journal of COPD. 2011. p. 413–21.

2. Spurzem JR, Rennard SI. Pathogenesis of COPD. Vol. 26, Seminars in Respiratory and Critical Care Medicine. 2005. p. 142–53.

3. Sharafkhaneh A, Hanania NA, Kim V. Pathogenesis of emphysema: From the bench to the bedside. Vol. 5, Proceedings of the American Thoracic Society. 2008. p. 475–7.

4. Kim V, Criner GJ. Chronic bronchitis and chronic obstructive pulmonary disease. Vol. 187, American Journal of Respiratory and Critical Care Medicine. 2013. p. 228–37.

5. Emphysema - PubMed - NCBI [Internet]. [cited 2019 Dec 26]. Available from: https://www.ncbi.nlm.nih.gov/pubmed/29489292

6. Laniado-Laborin R. Smoking and chronic obstructive pulmonary disease (COPD). Parallel epidemics of the 21st century. Vol. 6, International Journal of Environmental Research and Public Health. 2009. p. 209–24.

7. Boschetto P, Quintavalle S, Miotto D, Lo Cascio N, Zeni E, Mapp CE. Chronic obstructive pulmonary disease (COPD) and occupational exposures. Vol. 1, Journal of Occupational Medicine and Toxicology. BioMed Central; 2006. p. 11.

8. Cho YM, Lee J, Choi M, Choi WS, Myong JP, Kim HR, et al. Work-related COPD after years of occupational exposure. Ann Occup Environ Med. 2015 Feb

19;27(1).

9. Roth M. Pathogenesis of COPD. Part III. Inflammation in COPD. Vol. 12, International Journal of Tuberculosis and Lung Disease. 2008. p. 375–80.

10. Hogg JC, Chu F, Utokaparch S, Woods R, Elliott WM, Buzatu L, et al. The nature of small-airway obstruction in chronic obstructive pulmonary disease. N Engl J Med [Internet]. 2004 Jun 24 [cited 2020 Apr 4];350(26):2645–53. Available from: http://www.ncbi.nlm.nih.gov/pubmed/15215480

11. Pavord ID, Jones PW, Burgel PR, Rabe KF. Exacerbations of COPD. Vol. 11 Spec, International journal of chronic obstructive pulmonary disease. 2016. p. 21–30.

12. Ko FW, Chan KP, Hui DS, Goddard JR, Shaw JG, Reid DW, et al. Acute exacerbation of COPD. Respirology [Internet]. 2016 Oct [cited 2020 Jan 8];21(7):1152–65. Available from: http://doi.wiley.com/10.1111/resp.12780

13. Qureshi H, Sharafkhaneh A, Hanania NA. Chronic obstructive pulmonary disease exacerbations: Latest evidence and clinical implications. Vol. 5, Therapeutic Advances in Chronic Disease. 2014. p. 212–27.

14. Mantero M, Rogliani P, Di Pasquale M, Polverino E, Crisafulli E, Guerrero M, et al. Acute exacerbations of COPD: Risk factors for failure and relapse. Vol. 12, International Journal of COPD. Dove Medical Press Ltd.; 2017. p. 2687–93.

15. Dransfield MT, Kunisaki KM, Strand MJ, Anzueto A, Bhatt SP, Bowler RP, et al. Acute exacerbations and lung function loss in smokers with and without chronic obstructive pulmonary disease. Am J Respir Crit Care Med. 2017 Feb

1;195(3):324–30.

16. Li J, Sun S, Tang R, Qiu H, Huang Q, Mason TG, et al. Major air pollutants and risk of COPD exacerbations: A systematic review and meta-analysis. Vol. 11, International Journal of COPD. Dove Medical Press Ltd.; 2016. p. 3079–91.

17. Sethi S, Murphy TF. Infection in the Pathogenesis and Course of Chronic Obstructive Pulmonary Disease [Internet]. 2020 [cited 2020 Jan 8]. Available from: www.nejm.org

18. Kobayashi S, Fujinawa R, Ota F, Kobayashi S, Angata T, Ueno M, et al. A single dose of lipopolysaccharide into mice with emphysema mimics human Chronic obstructive pulmonary disease exacerbation as assessed by micro-computed tomography. Am J Respir Cell Mol Biol [Internet]. 2013 Dec [cited 2020 Apr 4];49(6):971–7. Available from: http://www.ncbi.nlm.nih.gov/pubmed/23822858

19. Tanabe N, Muro S, Hirai T, Oguma T, Terada K, Marumo S, et al. Impact of exacerbations on emphysema progression in chronic obstructive pulmonary disease. Am J Respir Crit Care Med. 2011 Jun 15;183(12):1653–9.

20. Wu J, Sin DD. Improved patient outcome with smoking cessation: When is it too late? Vol. 6, International Journal of COPD. Dove Press; 2011. p. 259–67.

21. Montuschi P. Pharmacological treatment of chronic obstructive pulmonary disease. Vol. 1, International journal of chronic obstructive pulmonary disease. 2006. p. 409–23.

22. Mei D, Shun W, Tan D, Shiu W, Wong F. Pharmacological strategies to regain steroid sensitivity in severe asthma and COPD. [cited 2020 Jan 8]; Available from:

https://doi.org/10.1016/j.coph.2019.04.010

23. Mukherjee M, Svenningsen S, Nair P. Glucocortiosteroid subsensitivity and asthma severity. Vol. 23, Current Opinion in Pulmonary Medicine. Lippincott Williams and Wilkins; 2017. p. 78–88.

24. Lopez-Campos JL, Carrasco Hernández L, Muñoz X, Bustamante V, Barreiro E. Current controversies in the stepping up and stepping down of inhaled therapies for COPD at the patient level. Vol. 23, Respirology. Blackwell Publishing; 2018. p. 818–27.

25. Poole PJ, Black PN. Mucolytic agents for chronic bronchitis or chronic obstructive pulmonary disease. Cochrane database Syst Rev [Internet]. 2000 [cited 2020 Jan 8];(2):CD001287. Available from: http://www.ncbi.nlm.nih.gov/pubmed/10796634

26. Starcher BC. Elastin and the lung. Thorax. 1986;41(8):577–85.

27. Shifren A, Mecham RP. The Stumbling Block in Lung Repair of Emphysema: Elastic Fiber Assembly. [cited 2020 Apr 3]; Available from: www.atsjournals.org

28. Suki B, Bartolák-Suki E, Rocco PRM. Elastase-induced lung emphysema models in mice. In: Methods in Molecular Biology [Internet]. Humana Press Inc.; 2017 [cited 2020 Apr 4]. p. 67–75. Available from: http://www.ncbi.nlm.nih.gov/pubmed/28752447

29. Faffe DS, Zin WA. Lung parenchymal mechanics in health and disease. Vol. 89, Physiological Reviews. American Physiological Society; 2009. p. 759–75.

30. Stoller JK, Aboussouan LS. α1-antitrypsin deficiency. In: Lancet [Internet]. 2005

[cited 2020 Apr 4]. p. 2225–36. Available from: http://www.ncbi.nlm.nih.gov/pubmed/15978931

31. Winkler T, Suki B. Emergent structure-function relations in emphysema and asthma. Crit Rev Biomed Eng [Internet]. 2011 [cited 2020 Apr 4];39(4):263–80. Available from: http://www.ncbi.nlm.nih.gov/pubmed/22011233

32. Luisetti M, Ma S, Iadarola P, Stone PJ, Viglio S, Casado B, et al. Desmosine as a biomarker of elastin degradation in COPD: Current status and future directions. Vol. 32, European Respiratory Journal. European Respiratory Society; 2008. p. 1146–57.

33. Labib S, Younes S, Riad E, Abdallah A. Study of blood desmosine level in patients with COPD exacerbation in relation to severity. Egypt J Chest Dis Tuberc. 2014 Jul 1;63(3):569–73.

34. Kim C, Ko Y, Kim SH, Yoo HJ, Lee JS, Rhee CK, et al. Urinary desmosine is associated with emphysema severity and frequent exacerbation in patients with COPD. Respirology [Internet]. 2018 Feb 1 [cited 2020 Apr 4];23(2):176–81. Available from: http://www.ncbi.nlm.nih.gov/pubmed/28905464

35. Sajjan U, Ganesan S, Comstock AT, Shim J, Wang Q, Nagarkar DR, et al. Elastase- and LPS-exposed mice display altered responses to rhinovirus infection. Am J Physiol - Lung Cell Mol Physiol. 2009 Nov;297(5).

36. Rushton L. Occupational causes of chronic obstructive pulmonary disease. Vol. 22, Reviews on Environmental Health. Walter de Gruyter GmbH; 2007. p. 195–212.

37. Kharitonov SA, Sjöbring U. Lipopolysaccharide Challenge of Humans as a Model for Chronic Obstructive Lung Disease Exacerbations. In: Models of Exacerbations in Asthma and COPD [Internet]. Basel: KARGER; 2007 [cited 2020 Apr 4]. p. 83–100. Available from: https://www.karger.com/Article/FullText/107056

38. Michel O, Duchateau J, Plat G, Cantinieaux B, Hotimsky A, Gerain J, et al. Blood inflammatory response to inhaled endotoxin in normal subjects. Clin Exp Allergy [Internet]. 1995 Jan [cited 2020 Apr 4];25(1):73–9. Available from: http://www.ncbi.nlm.nih.gov/pubmed/7728626

39. Brass DM, Hollingsworth JW, Cinque M, Li Z, Potts E, Toloza E, et al. Chronic LPS inhalation causes emphysema-like changes in mouse lung that are associated with apoptosis. Am J Respir Cell Mol Biol. 2008 Nov 1;39(5):584–90.

40. Lee S-Y, Cho J-H, Cho SS, Bae C-S, Kim G-Y, Park D-H. Establishment of a chronic obstructive pulmonary disease mouse model based on the elapsed time after LPS intranasal instillation. Lab Anim Res [Internet]. 2018 Mar [cited 2020 Apr 4];34(1):1. Available from: http://www.ncbi.nlm.nih.gov/pubmed/29628971

41. Kaneko Y, Takashima K, Suzuki N, Yamana K. Effects of theophylline on chronic inflammatory lung injury induced by LPS exposure in guinea pigs. Allergol Int [Internet]. 2007 Dec [cited 2020 Apr 4];56(4):445–56. Available from: http://www.ncbi.nlm.nih.gov/pubmed/17965584

42. Dupont A, Dury S, Gafa V, Lebargy F, Deslée G, Guenounou M, et al. Impairment of neutrophil reactivity to elastin peptides in COPD. Thorax. 2013 May 1;68(5):421–8.

43. Corhay JL, Moermans C, Henket M, Dang DN, Duysinx B, Louis R. Increased of exhaled breath condensate neutrophil chemotaxis in acute exacerbation of COPD. Respir Res. 2014 Sep 28;15(1).

44. Wu J, Hillier C, Komenda P, Lobato de Faria R, Levin D, Zhang M, et al. A Microfluidic Platform for Evaluating Neutrophil Chemotaxis Induced by Sputum from COPD Patients. Proost P, editor. PLoS One [Internet]. 2015 May 11 [cited 2020 May 30];10(5):e0126523. Available from: https://dx.plos.org/10.1371/journal.pone.0126523

45. Yoshikawa T, Dent G, Ward J, Angco G, Nong G, Nomura N, et al. Impaired neutrophil chemotaxis in chronic obstructive pulmonary disease. Am J Respir Crit Care Med. 2007 Mar 1;175(5):473–9.

46. Segura-Valdez L, Pardo A, Gaxiola M, Uhal BD, Becerril C, Selman M. Upregulation of gelatinases A and B, collagenases 1 and 2, and increased parenchymal cell death in COPD. Chest. 2000;117(3):684–94.

47. Kasahara Y, Tuder RM, Cool CD, Lynch DA, Flores SC, Voelkel NF. Endothelial cell death and decreased expression of vascular endothelial growth factor and vascular endothelial growth factor receptor 2 in emphysema. Am J Respir Crit Care Med. 2001;163(3 I):737–44.

48. Imai K, Mercer BA, Schulman LL, Sonett JR, D'Armiento JM. Correlation of lung surface area to apoptosis and proliferation in human emphysema. Eur Respir J. 2005 Feb;25(2):250–8.

49. Makris D, Vrekoussis T, Izoldi M, Alexandra K, Katerina D, Dimitris T, et al.

Increased apoptosis of neutrophils in induced sputum of COPD patients. Respir Med. 2009 Aug;103(8):1130–5.

50. Dunnill MS. Quantitative methods in the study of pulmonary pathology. Thorax [Internet]. 1962 [cited 2020 Jun 29];17(4):320–8. Available from: https://www.ncbi.nlm.nih.gov/pmc/articles/PMC1018718/

51. Knudsen L, Weibel ER, Gundersen HJG, Weinstein F V., Ochs M. Assessment of air space size characteristics by intercept (chord) measurement: An accurate and efficient stereological approach. J Appl Physiol [Internet]. 2010 Feb [cited 2020 Jun 29];108(2):412–21. Available from: https://pubmed.ncbi.nlm.nih.gov/19959763/

52. Hasleton PS. The internal surface area of the adult human lung. J Anat [Internet]. 1972 Sep [cited 2020 Jun 29];112(Pt 3):391–400. Available from: http://www.ncbi.nlm.nih.gov/pubmed/4564685

53. Cantor J, Ochoa A, Ma S, Liu X, Turino G. Free Desmosine is a Sensitive Marker of Smoke-Induced Emphysema. Lung. 2018 Dec 1;196(6):659–63.

54. Kim V, Aaron SD. What is a COPD exacerbation? Current definitions, pitfalls, challenges and opportunities for improvement. Eur Respir J. 2018;52(5).

55. Hurst JR, Vestbo J, Anzueto A, Locantore N, Müllerova H, Tal-Singer R, et al. Susceptibility to Exacerbation in Chronic Obstructive Pulmonary Disease. N Engl J Med [Internet]. 2010 Sep 16 [cited 2020 Jun 3];363(12):1128–38. Available from: http://www.nejm.org/doi/abs/10.1056/NEJMoa0909883

56. Donaldson GC, Seemungal TAR, Bhowmik A, Wedzicha JA. Relationship

between exacerbation frequency and lung function decline in chronic obstructive pulmonary disease. Thorax. 2002 Oct 1;57(10):847–52.

57. Niewoehner DE, Erbland ML, Deupree RH, Collins D, Gross NJ, Light RW, et al. Effect of systemic glucocorticoids on exacerbations of chronic obstructive pulmonary disease. N Engl J Med. 1999 Jun 24;340(25):1941–7.

58. Barr RG, Rowe BH, Camargo CA. Methylxanthines for exacerbations of chronic obstructive pulmonary disease. Cochrane Database Syst Rev. 2003 Apr 22;327(7416):643–6.

59. MacNee W, Calverley PMA. Chronic obstructive pulmonary disease • 7: Management of COPD. Vol. 58, Thorax. BMJ Publishing Group Ltd; 2003. p. 261–5.

60. Suki B, Stamenovic D, Hubmayr R. Lung Parenchymal Mechanics. 2011;

61. Kononov S, Brewer K, Sakai H, Cavalcante FSA, Sabayanagam CR, Ingenito EP, et al. Roles of mechanical forces and collagen failure in the development of elastase-induced emphysema. Am J Respir Crit Care Med. 2001 Nov 15;164(10 I):1920–6.

62. Hogg JC, Timens W. The Pathology of Chronic Obstructive Pulmonary Disease. Annu Rev Pathol Mech Dis [Internet]. 2009 Feb [cited 2020 Apr 5];4(1):435–59. Available from: http://www.ncbi.nlm.nih.gov/pubmed/18954287

63. Tuder RM, Petrache I. Pathogenesis of chronic obstructive pulmonary disease. Vol. 122, Journal of Clinical Investigation. American Society for Clinical Investigation; 2012. p. 2749–55.

64. Suki B, Bates JHT. Lung tissue mechanics as an emergent phenomenon. J Appl Physiol. 2011 Apr 1;110(4):1111–8.

65. MacNee W. Pathogenesis of chronic obstructive pulmonary disease. In: Proceedings of the American Thoracic Society. Proc Am Thorac Soc; 2005. p. 258–66.

66. Bathoorn E, Kerstjens HAM, Postma D, Timens W, MacNee W. Airways inflammation and treatment during acute exacerbations of COPD. Vol. 3, International Journal of COPD. Int J Chron Obstruct Pulmon Dis; 2008. p. 217–29.

67. Hoenderdos K, Condliffe A. The neutrophil in chronic obstructive pulmonary disease: Too little, too late or too much, too soon? Vol. 48, American Journal of Respiratory Cell and Molecular Biology. Am J Respir Cell Mol Biol; 2013. p. 531–9.

68. Ma S, Turino GM, Lin YY. Quantitation of desmosine and isodesmosine in urine, plasma, and sputum by LC-MS/MS as biomarkers for elastin degradation. J Chromatogr B Anal Technol Biomed Life Sci [Internet]. 2011 Jul 1 [cited 2020 Apr 5];879(21):1893–8. Available from: http://www.ncbi.nlm.nih.gov/pubmed/21621489

69. Fregonese L, Ferrari F, Fumagalli M, Luisetti M, Stolk J, Iadarola P. Long-term variability of desmosine/isodesmosine as biomarker in alpha-1-antritrypsin deficiencyrelated COPD. COPD J Chronic Obstr Pulm Dis [Internet]. 2011 Oct [cited 2020 Apr 5];8(5):329–33. Available from: http://www.ncbi.nlm.nih.gov/pubmed/21793711

70. Ma S, Lin YY, Cantor JO, Chapman KR, Sandhaus RA, Fries M, et al. The Effect of Alpha-1 Proteinase Inhibitor on Biomarkers of Elastin Degradation in Alpha-1 Antitrypsin Deficiency: An Analysis of the RAPID/RAPID Extension Trials. Chronic Obstr Pulm Dis J COPD Found [Internet]. 2017 Nov 18 [cited 2020 Apr 5];4(1):34–44. Available from: http://www.ncbi.nlm.nih.gov/pubmed/28848909

71. Joddar B, Ramamurthi A. Elastogenic effects of exogenous hyaluronan oligosaccharides on vascular smooth muscle cells. Biomaterials. 2006 Nov;27(33):5698–707.

72. Deslee G, Woods JC, Moore CM, Liu L, Conradi SH, Milne M, et al. Elastin expression in very severe human COPD. Eur Respir J. 2008 Aug;34(2):324–31.

73. Balkissoon R. Stem Cell Therapy for COPD: Where are we? Chronic Obstr Pulm Dis J COPD Found. 2018;5(2):148–53.

74. Hind M, Maden M. Is a regenerative approach viable for the treatment of COPD? Vol. 163, British Journal of Pharmacology. Wiley-Blackwell; 2011. p. 106–15.

75. Houghton AM, Quintero PA, Perkins DL, Kobayashi DK, Kelley DG, Marconcini LA, et al. Elastin fragments drive disease progression in a murine model of emphysema. J Clin Invest [Internet]. [cited 2020 Apr 5]; Available from: http://www.jci.org

76. Hunninghake GW, Davidson JM, Rennard S, Szapiel S, Gadek JE, Crystal RG. Elastin fragments attract macrophage precursors to diseased sites in pulmonary emphysema. Science (80-) [Internet]. 1981 May 22 [cited 2020 Apr 5];212(4497):925–7. Available from:

http://www.ncbi.nlm.nih.gov/pubmed/7233186

77. Sellami M, Meghraoui-Kheddar A, Terryn C, Fichel C, Bouland N, Diebold MD, et al. Induction and regulation of murine emphysema by elastin peptides. Am J Physiol - Lung Cell Mol Physiol [Internet]. 2016 Jan 1 [cited 2020 Apr 5];310(1):L8–23. Available from: http://www.ncbi.nlm.nih.gov/pubmed/26519205

78. Gamble E, Grootendorst DC, Hattotuwa K, O'shaughnessy T, Ram FSF, Qiu Y, et al. Airway mucosal inflammation in COPD is similar in smokers and ex-smokers: a pooled analysis. Eur Respir J [Internet]. 2007 [cited 2020 Apr 5];30(3):467–71. Available from: www.erj.ersjournals.com/misc/statements.shtml

79. Kheradmand F, Shan M, Xu C, Corry DB. Autoimmunity in chronic obstructive pulmonary disease: clinical and experimental evidence. Expert Rev Clin Immunol. 2012;8(3):285–92.

80. Cantor JO, Shteyngart B, Cerreta JM, Liu M, Armand G, Turino GM. The Effect of Hyaluronan on Elastic Fiber Injury In Vitro and Elastase-Induced Airspace Enlargement In Vivo. Proc Soc Exp Biol Med. 2000 Oct;225(1):65–71.

81. Cantor JO, Cerreta JM, Ochoa M, Ma S, Chow T, Grunig G, et al. Aerosolized hyaluronan limits airspace enlargement in a mouse model of cigarette smoke-induced pulmonary emphysema. Exp Lung Res [Internet]. 2005 May [cited 2020 Apr 10];31(4):417–30. Available from: http://www.ncbi.nlm.nih.gov/pubmed/16025922

82. Cantor J, Ma shuren, Turino gerard. COPD-142156-a-pilot-clinical-trial-to-determine-the-safety-and-efficacy-. Int J COPD [Internet]. 2017 [cited 2020 Apr

10];2017:12–2747. Available from: http://dx.doi.org/10.2147/COPD.S142156

83. Kaur M, Singh D. Neutrophil chemotaxis caused by chronic obstructive pulmonary disease alveolar macrophages: The role of CXCL8 and the receptors CXCR1/CXCR2. J Pharmacol Exp Ther. 2013 Oct;347(1):173–80.

84. Plataki M, Tzortzaki E, Rytila P, Demosthenes M, Koutsopoulos A, Siafakas NM. Apoptotic mechanisms in the pathogenesis of COPD. Vol. 1, International journal of chronic obstructive pulmonary disease. Dove Press; 2006. p. 161–71.

Vita

Name	Shadi Mehraban
Degrees and Certificates	*Doctor of Medicine, Jahrom University of Medical Sciences, Jahrom, Iran* *Major: Medicine*
Date Graduated	*08/2015*